China Ocean Eng., Vol. 30, No. 6, pp. 967 – 978

DOI 10.1007/s13344-016-0063-1, ISSN 0890-5487

Experimental Investigation of Wave Slamming on An Open Structure Supported Elastically*

REN Bing (任 冰)[a, 1], LIU Ming (刘 明)[a],

LI Xue-lin (李雪临)[b] and WANG Yong-xue (王永学)[a]

[a] *State Key Laboratory of Coastal and Offshore Engineering*, *Dalian University of Technology*, *Dalian 116024*, *China*

[b] *Department of Marine Strategy Research & Planning*, *National Ocean Technology Center*, *State Oceanic Administration*, *Tianjin 300112*, *China*

(Received 20 March 2015; received revised form 22 September 2015; accepted 16 November 2015)

ABSTRACT

The superstructures of marine structures supported by the elastic legs and located in the splash zone will subject to violent wave slamming and vibrate consequently during storms. A series of model tests are carried out to investigate the wave impacting on the open structures supported elastically. Three kinds of models with different natural frequencies are designed. The characteristics of the wave pressures on the three models are compared. The durations of the uplift forces and the corresponding accelerations of the structure during wave impact are analyzed simultaneously. The distributions of the peak impact pressures on the subfaces of the plates with different supporting stiffness are given. The relationship between the uplift force on the three models and the relative clearance are obtained. The spectral properties of the slamming loads on the three different structures are compared. The experimental results indicate that the behaviors of the impact pressures, the uplift forces and accelerations of the plates with small natural frequencies are obviously different from those of the plates with larger natural frequencies within the range of the experimental parameters.

Key words: *supported elastically*; *wave impact*; *acceleration*; *hydro-elasticity*

1. Introduction

Wave impact (slamming) is a violent wave-structure interaction, where different physical effects such as air cushion, compressibility of the water and the dynamic hydroelastic effects may be relevant. The superstructure of marine structures (such as open sea terminal, marine trestle and offshore platform) is usually subject to violent wave impacting under rough sea conditions. Previous studies find that wave impact is often accompanied with large deformation of free surface and high-frequency slamming loads. The great impact loads often lead to the partial damage or the entire collapse of the structure. For the elastic systems, the wave-induced vibrations give rise to the structure failure.

The water entry method pioneered by von Kármán (1929) and Wagner (1932) is used to describe a

* This work was financially supported by the National Natural Science Foundation of China (Grant No. 51179030) and the Innovative Research Group National Natural Science Foundation of China (Grant No. 51309056).

1 Corresponding author. E-mail: bren@dlut.edu.cn

nearly horizontal free surface impacting the deck. Though Wagner's theory assumes small local deadrise angle and potential flow, it provides the simple analytical results of the slamming forces on the two-dimensional body. The difference between the von Karman's and Wagner's methods is that the von Karman's method neglects the local uprise of the water when calculating the wetted surface. According to Faltinsen (2009), Wagner's flat plate assumption is suitable for small deadrise angles and von Karman's solution underestimates the water entry force for small deadrise angles, whereas the generalized Wagner's solution (Zhao, 1996) is good for large deadrise angles.

For wave impacting on the horizontal members located in the splash zone, the analytical solution to wave entry of small horizontal cylinders is taken to calculate the wave impact force $F_i = \frac{1}{2} C_s \rho U^2 D l$. The slamming coefficient C_s is taken as π using von Karman's method, whereas C_s=2π using the Wagner's method accounting for the rise of water. The slamming coefficient C_s yielded by the experiments exhibits a considerable degree of scatter, ranging from about 1.0 to 6.4 (Miller, 1978; Faltinsen, 1977; Sarpkaya, 1978). Kaplan (1976) presented the slamming forces on the small horizontal cylinders with the similar form of Morrison formula based on the momentum theorum. Kaplan (1992) extended the methods dealing with the small horizontal cylinders to large platforms and presented the analytical solution of vertical slamming forces. Kaplan's treatment neglected the influence of wave deformation and wave breaking. Baarholm (2000) presented an approximate solution for wave impact on a fixed horizontal deck based on Wagner's solution. The above theoretical results assume an irrotational flow of inviscid water and have difficult in dealing with complicated flows with the broken waves and overturn surfaces.

Many researchers carried out a series of experiments (Faltinsen, 1975; Abramson, 1976; Goda, 1967) to investigate the wave slamming. Water-entry experiments of small horizontal cylinder are used to model impact forces on the horizontal members of superstructures (Sarpkaya, 1978). Baarholm (2000) and Ren *et al.* (2005) made experimental investigations of wave impacting on the large horizontal plates. With the development of Computational Fluid Dynamics (CFD), varieties of numerical methods have been applied to simulate wave impact on marine structures (Ren *et al.*, 2004).

Wave impacting causes the elastic vibrations of the structure. The hydroelasticity may be important and affect the hydrodynamic loads, which means that hydrodynamic condition and the elastic response should be considered simultaneously. Faltinsen (1997, 1999) investigated water entry of an elastic structure with a wedge cross section of different deadrise angles. The experimental statement is that the hydroelasticity should be considered for the deadrise angle samller than 5°. Faltinsen (2000) and Korobkin (1999) examined the hydroelasticity relevance for horizontal structures made with steel and aluminum, where the structure was dropped on the free surface. The structure was modeled as a beam, and the impact loads were calculated by the generalization of Wagner's method including the effect of elastic vibrations. Sumi (1997) carried out experiments to study water-entry impact of elastic plate with small deadrise angles. Tanizawa (1998) presented a time-domain simulation by Boundary Element Method (BEM) to study water-entry of two-dimensional elastic beam with a constant velocity. There are significant differences between the hydroelastic slamming of ocean structure and the water-entry of

elastic plates mentioned above. For instance, for the jacket platform, the superstructure with large stiffness can be considered as a rigid body, the support legs with smaller stiffness should be regarded as elastic support. Sulisz (2005, 2008) carried out model tests to study the wave impact on an elastically supported plate. The features of structure vibrations in four different stages are found. At present about the studies on wave impact on open structures with elastic support have rarely been reported. Efforts should be made towards the influence of hydroelasticity on the impact pressures as well as the mutual interaction between the fluid flow and the elastic response of the structure.

In this study the experiments are carried out to investigate the wave impacting on the elastically supported structures. Three kinds of models with different natural frequencies are designed. The characteristics of the wave pressures on the three different models are compared. The distributions of the peak impact pressures on the subfaces of different models are given. The durations of the uplift forces and the accelerations of the structure during one wave impact period are analyzed simultaneously. The relationship between the uplift forces and the relative clearance is discussed. The spectrum properties of the slamming loads on the three different structures are compared.

2. Experimental Set-up

The experiments were conducted in the wave flume of the State Key Laboratory of Coastal and Offshore Engineering (SLCOE) in Dalian University of Technology (DUT). The wave flume is 22 m long, 0.8 m wide and 0.8 m deep. It is equipped with a wave maker of hydraulic-servo type on the left side, which is driven by a piston-type system and equipped with a data acquisition system. At the far end of the tank, a wave energy dissipation device is set to attenuate the reflected wave. The structure model was centrally installed in the mid-back part of the tank, as shown in Fig. 1.

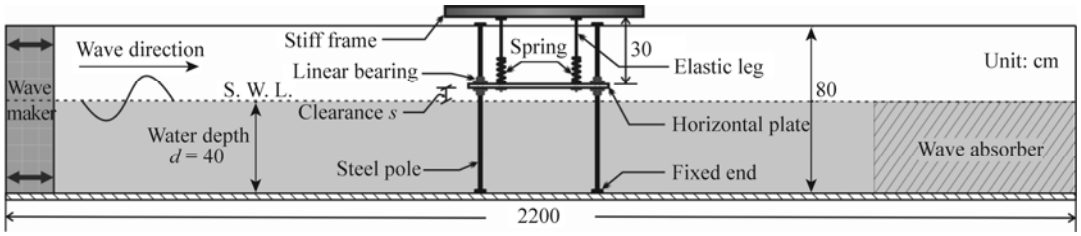

Fig. 1. General layout of the wave flume.

The test model was simplified as an elastically supported plate with one degree of freedom. The plate was made of 12 mm thick acrylic with 0.78 m in length and 0.78 m in width. The plate was suspended above the water surface by a supporting device with one end fixed to the plate and the other to a bracket placed on the top of the tank, as shown in Fig. 2. Four springs were used to connect the plate and the supporting steel wires (12 mm in the diameter). Another four steel poles and linear bearings were used to limit the movement of the plate, which could only move vertically. The connecting points of the springs to the plate were defined by M1, … , M4. The connecting points of the steel poles to the plate were defined as L1, … , L4, respectively, as shown in Fig. 3.

Three kinds of models with different supporting stiffness were tested. The diameters of connecting springs of Model01 and Model02 were 4 mm and 6 mm, and the corresponding stiffness coefficients k_1 and k_2 were 1605 N/m and 4704 N/m, respectively. The plate of Model03 was connected with the steel wire without a spring. The elastic modulus of the steel wire was 2.0×10^5 MPa. The distance between the plate and the bracket on the top of the tank was 30 cm when the plate was in the equilibrium position.

The natural frequencies f and the damping ratios ξ of the three models were measured with the initial displacement method, as listed in Table 1. The model vibrated freely in the air under an initial displacement. The acceleration data were collected by the accelerometer. The natural frequency and the vertical stiffness were obtained by the spectral analysis of the time series of acceleration. The damping ratio was determined by the amplitudes ratio of the two neighboring peaks in the time series of acceleration. It can be seen from Table 1 that the stiffness of Model03 is very large and can be treated as a rigid body.

Eight pressure transducers P1,…, P8 and two accelerometers A1, A2 were installed on the subface of the model plate, as shown in Fig. 3. The hydrodynamic pressures and acceleration signals were measured simultaneously using a CRIO-9074, 32-channel synchronous acquisition instrument, which was fabricated by the National Instruments (NI). The sampling interval in the test was 1/1000 s.

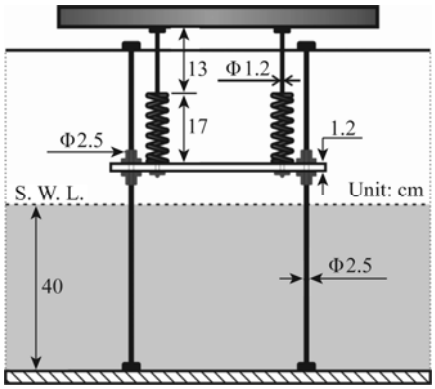

Fig. 2. Sketch of the test model.

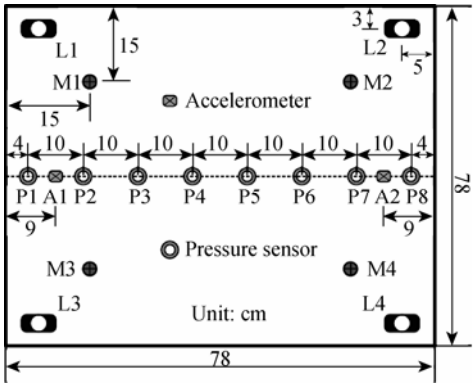

Fig. 3. Arrangement of pressure sensors and accelerometers.

Table 1 Parameters of free vibration of the models

Test model	Deck mass M (kg)	Elastic coefficient k (kN/m)	Natural frequency f (Hz)	Damping ratio ξ
Model01	8.8	7.32	4.6	0.23
Model02	8.8	19.50	7.5	0.20
Model03	8.8	465.00	36.6	0.08

The incident waves were regular waves and the water depth (d) was 0.40 m. Wave height (H) ranged from 8.0 cm to 12.0 cm. Wave periods (T) were chosen from 1.0 s to 1.6 s. The relative clearance (s/H) ranged from 0.0 to 0.4.

Fig. 4 shows the measured time series and spectral analysis results of the incident wave surface elevation at the position of the structure model. It can be seen in Fig. 4 that the measured incident waves have higher and steeper wave crests as well as shallower and flatter wave troughs. The wave surface

profiles show a significant asymmetry. The amplitude spectra of the wave surface elevations indicate that the main peaks arise at the incident wave frequencies and the secondary peak arises at the double incident wave frequencies. For the case of T=1.3 s and H=12 cm, the frequencies are 0.77 Hz and 1.54 Hz, respectively. The corresponding peak values are 5.6 cm and 1.2 cm, respectively. Though the target waves are set as single phase waves, the measured incident waves have two components of different frequencies and significant nonlinearity.

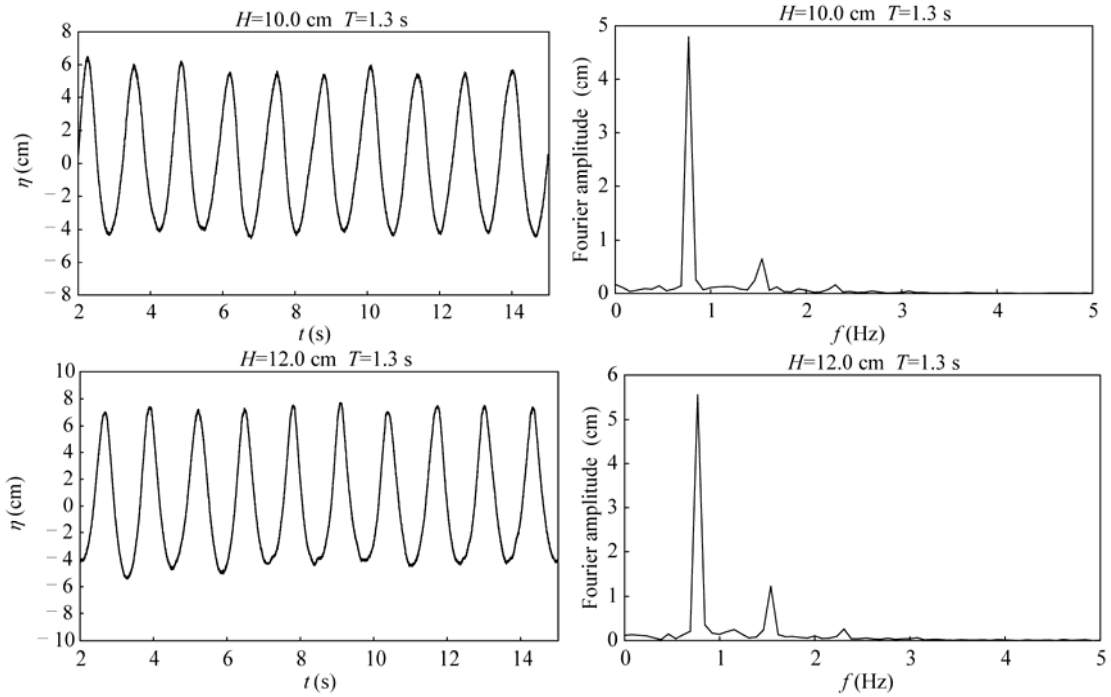

Fig. 4. Time series and amplitude spectra of incident wave surface elevations.

3. Experimental Results

3.1 Wave Impact Pressure

Fig. 5 shows the time series of pressures on the measured point P1 for the three test models (T=1.3 s, H=12 cm, s/H=0.2). It can be seen from Fig. 5 that a peak pressure occurs with a large magnitude and very short duration firstly, followed by a positive hydrodynamic pressure with a long duration. Then the hydrodynamic pressure decreases to a negative value. Finally when the water is separated from the underside of the plate, the pressure is zero.

It can be seen that the slamming duration is significantly different for the different models. For the model with the largest stiffness (k=465 kN/m), the peak pressure occurs at the moment of contacting, and the duration of slamming is about 0.64 s. For the other two models with smaller stiffness (k=19.5 kN/m and k=7.32 kN/m), the peak pressure lags slightly behind the contacting moment. And the durations for these two cases are about 0.90 s and 0.72 s, respectively.

The models with different stiffness move differently under the impact of the same wave conditions.

When the waves impact on the plates, the models with smaller stiffness move up under the impact action. Thus, the peak pressure lags behind the impacting moment. And the amplitudes of the movements are larger for the models with smaller stiffness, therefore, the durations of the interaction between the plates and the waves are longer, which results in the longer impacting durations. However, for the model with large stiffness, the moving amplitude is very small and the property of the impact pressure is similar to that on the rigid body. That is, the peak pressure occurs at the impacting moment (Ren, 2005).

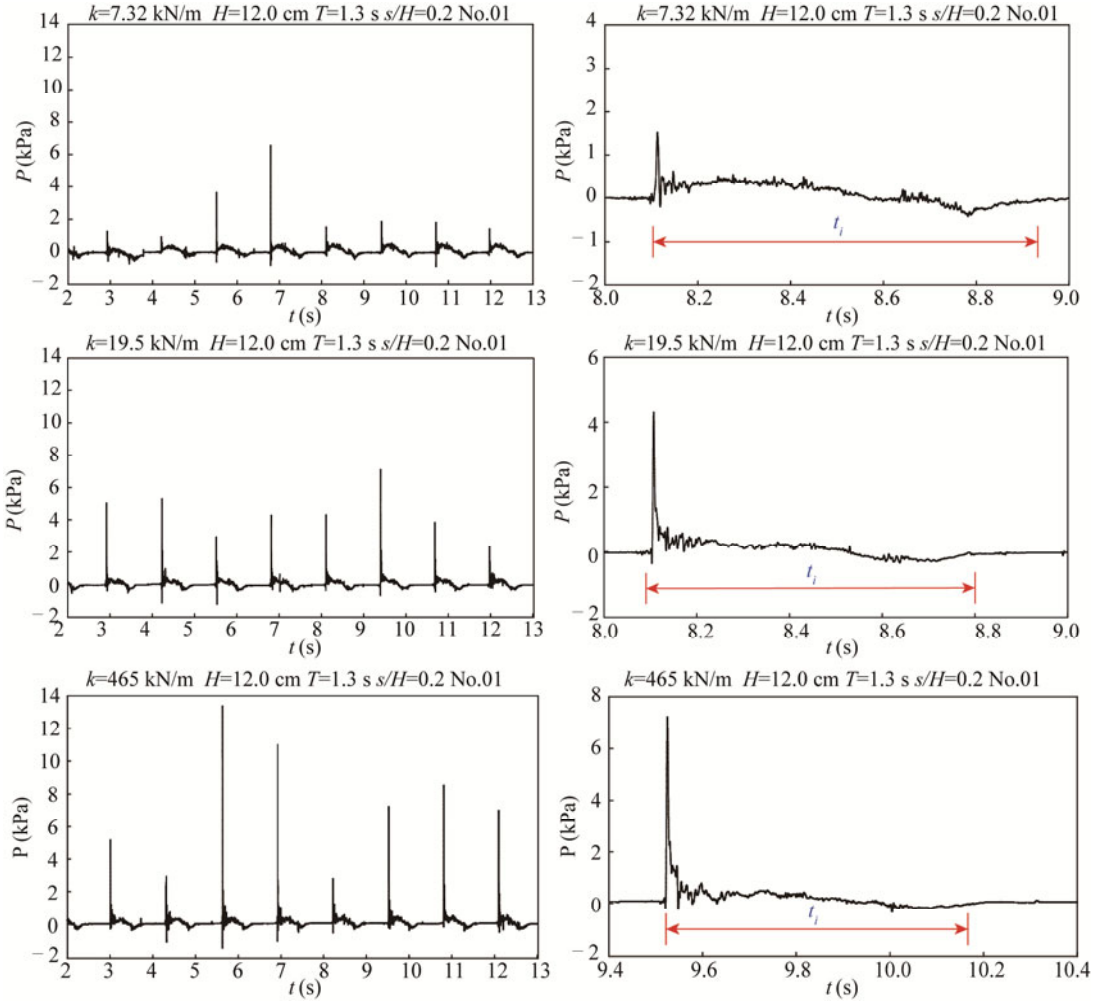

Fig. 5. Time series of the wave impact pressures of P1 (T=1.3 s, H=12 cm, s/H=0.2).

3.2 Synchronous Analysis of the Uplift Force and the Acceleration

The synchronous time series of uplift forces and accelerations for three alternative test models are shown in Fig. 6 (T=1.3 s, H=12 cm, s/H=0.2). The uplift forces are obtained by integrating the pressures of the eight measured points and the representative area of each point. The accelerations of the model are calculated as the mean of the accelerations recorded by gauges A1 and A2.

It can be seen from Fig. 6 that properties of the uplift forces are similar to those of the impact pressures. That is to say that a peak force of a large magnitude and a short duration arises when waves are contacting the subface of the model. Then a hydrodynamic force with a longer duration occurs. Finally, when the wave separates from the model, the force changes to zero.

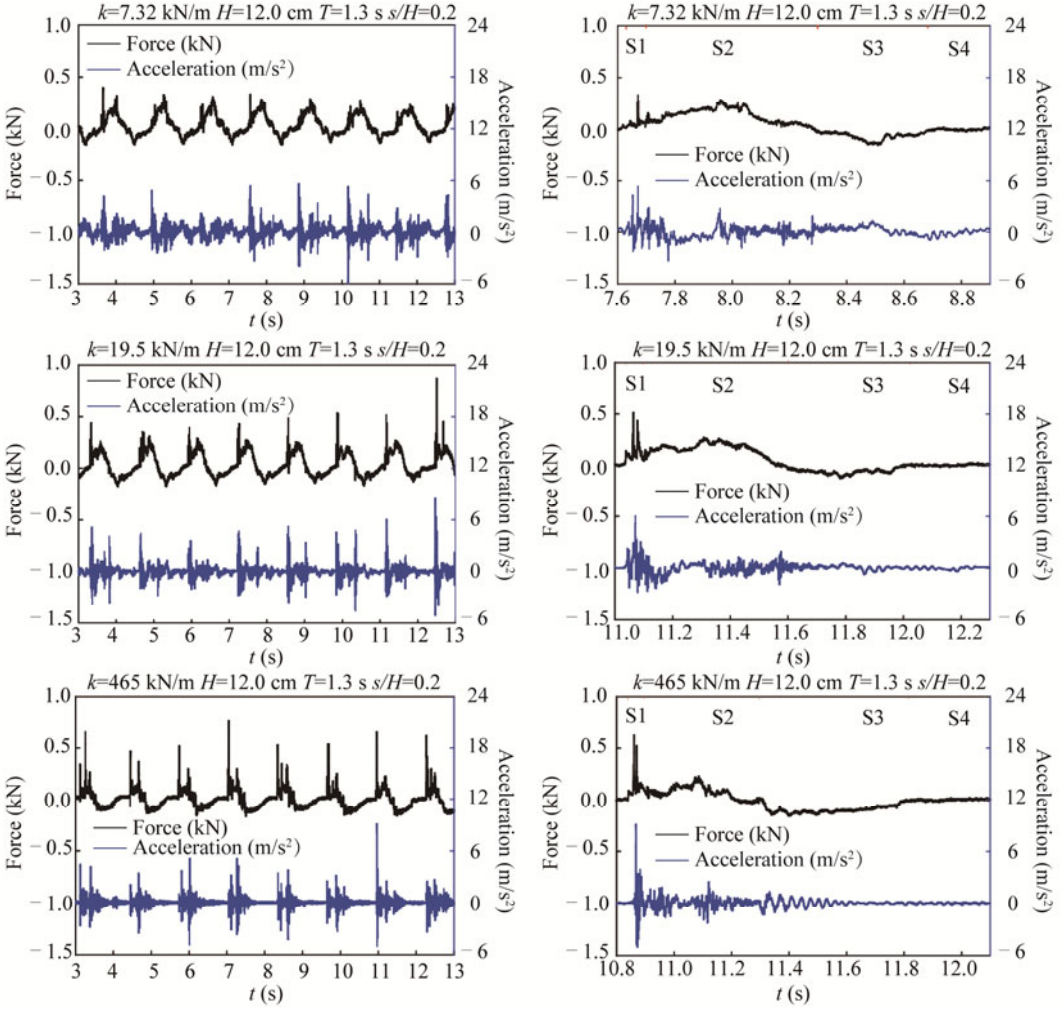

Fig. 6. Synchronous duration histories of the uplift forces and accelerations (T=1.3 s, H=12 cm, s/H=0.2).

From the synchronous analysis of the uplift force and the acceleration, it is concluded that one wave slamming period can be divided into four stages: the initial stage of waves contacting the underside of the model, the structure submerged by the water, the water shedding from structure, the water completely separated from the underside of the model, which are denoted by S1–S4 in turn. The duration of the first stage (S1) is very short, where a peak pressure of a very high magnitude induced by the violent instantaneous interaction between the water and the structure occurs. The corresponding acceleration with relatively large amplitude oscillates violently. The duration of S2 is longer, the hydrodynamics

pressure is relevant with the immersed part of the structure by the water, where the acceleration still oscillates violently with a smaller amplitude than that of S1. In the stage of S3, the water begins to separate from the structure and the wave force transforms from the positive to the negative value. The acceleration of S3 is very small with little oscillation. In the stage of S4, the water separates from the structure completely. The wave force becomes zero and the acceleration gradually changes to zero, where the structure vibrates freely. The characteristics of the acceleration in each stage are similar to the conclusion of Sulisz (2005).

By comparing the three models it can be seen that for the model with larger stiffness, the oscillating amplitude of the acceleration is relatively small, especially in the stage of free vibration, the acceleration changes to zero rapidly due to its higher natural frequency. For the model with smaller stiffness, the acceleration oscillates more violently in each stage.

3.3 Effects of Supporting Stiffness on Wave Impact Loads

It can be seen from the time series of pressures shown in Fig. 5 that the occurrence frequency of large amplitude impacting pressure on the model with smaller stiffness is lower than that of the model with larger stiffness. For the case of k=464.9 kN/m, the peak pressure with a large amplitude occurs in every impacting period and the amplitude of the peak pressure is obviously larger than that of the other two cases (k=7.32 kN/m, and k=19.5 kN/m). The effect of the supporting stiffness on the impact pressures is similar to that on the impact forces as shown in Fig. 6.

The distributions of the peak impact pressures on the subfaces of the three models are given in Fig. 7. The abscissa is the number of measured points n (see Fig. 2). The ordinate is the average peak pressures P_c. It can be seen from Fig. 7 that the impacting pressures distribute uniformly for the model with smaller stiffness (k=7.32 kN/m), whereas for the models with larger stiffness (k=19.5 kN/m and k=465 kN/m) the peak pressures of P2 and P3 on the seaward are obviously larger than that of the measured points on the shoreward. The peak pressures of P1–P3 on the seaward increase with the increase of the supporting stiffness, whereas the peak pressures of P4–P8 on the shoreward change little with the increase of the supporting stiffness.

Fig. 8 shows the relationships between the peak forces and the relative clearance for the three models. The ordinate is the average peak impact forces F_c. It can be seen that in this experiment, the peak forces increase with the increase of the supporting stiffness for the same incident waves and clearance. The study of wave slamming on the rigid body shows that the maximum value of the impact forces occurs at a certain relative clearance instead of s/H=0 (Ren, 2005). It can be seen from Fig. 8 that for the models of k=465 kN/m and k=19.5 kN/m, the maximum value of the peak force occurs at s/H=0.1–0.2, which is similar to the rigid case. For the model with smaller stiffness (k=7.32 kN/m), the impact peak force is small and changes little with the change of the relative clearance. The possible reason is that for the model with small supporting stiffness, the amplitude of the model's movenment is large in the case of small clearance, which makes the actual clearacne large. At the case of large clearance, the amplitude of the model's movement is small, thus, the actual clearance changes littile, which makes the impact force change little with the change of the clearance.

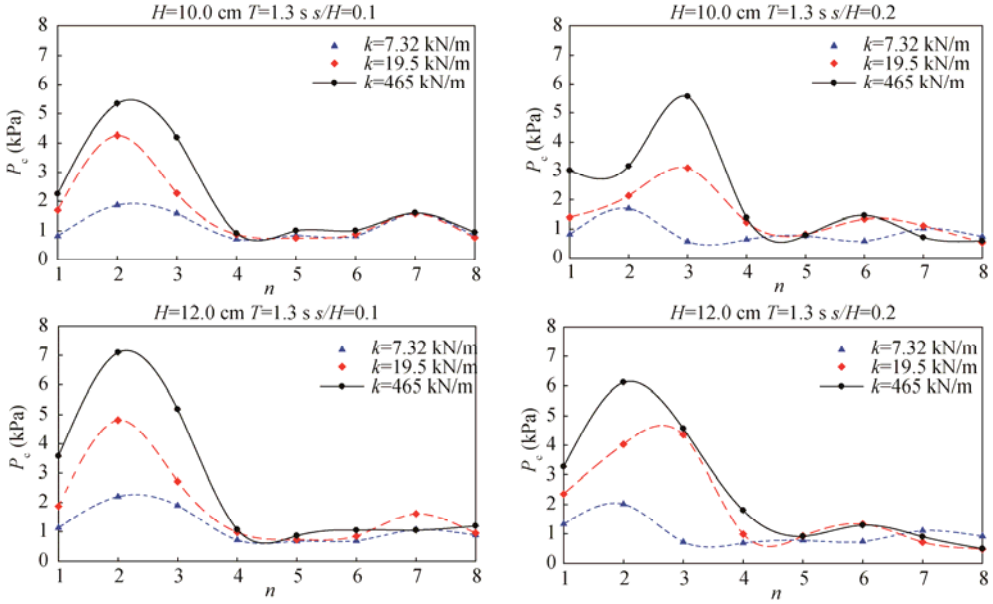

Fig. 7. Distribution of the peak pressures on the subfaces of the structures with different supporting stiffness.

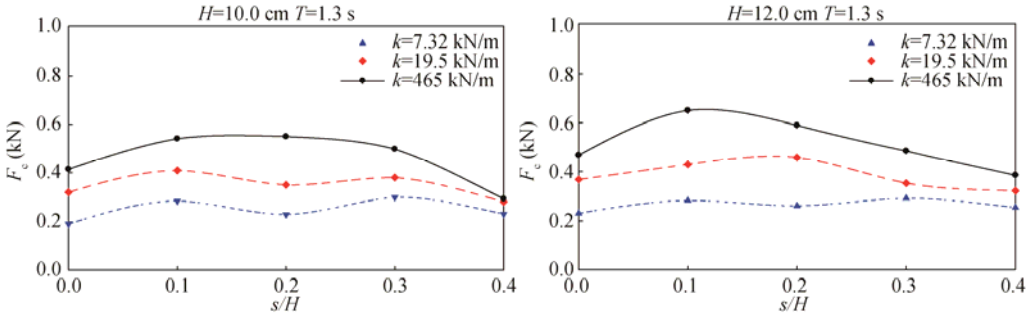

Fig. 8. Relationship between the peak forces and the relative clearance.

3.4 Spectral Analysis of Wave Impact Loads

Fig. 9 shows the amplitude spectra of impact pressures of P2 (left) and uplift forces (right) (T=1.3 s, H=12 cm). As it can be seen from Fig. 9, for the pressure spectrum and the force spectrum, a very high main peak arises at the incident wave frequency (f=0.77 Hz) and secondary peaks with smaller amplitudes arise at the double frequency and triple frequency. The maximum value of the main peak at the incident frequency occurs at s/H=0.0, whereas the maximum value of the secondary peak at the double frequency occurs at s/H=0.2. As the clearance increases, the difference between the main peak and the secondary peak becomes smaller. When the relative clearance s/H=0.4, the difference is very tiny. Owing to the incident wave's significant nonlinearity and its two components of different frequencies (as shown in Fig. 4), it is the wave crest acting on the structure when impacting happens. Especially when the clearance of the structure is larger, the acting part with the structure is the higher order components of the incident waves.

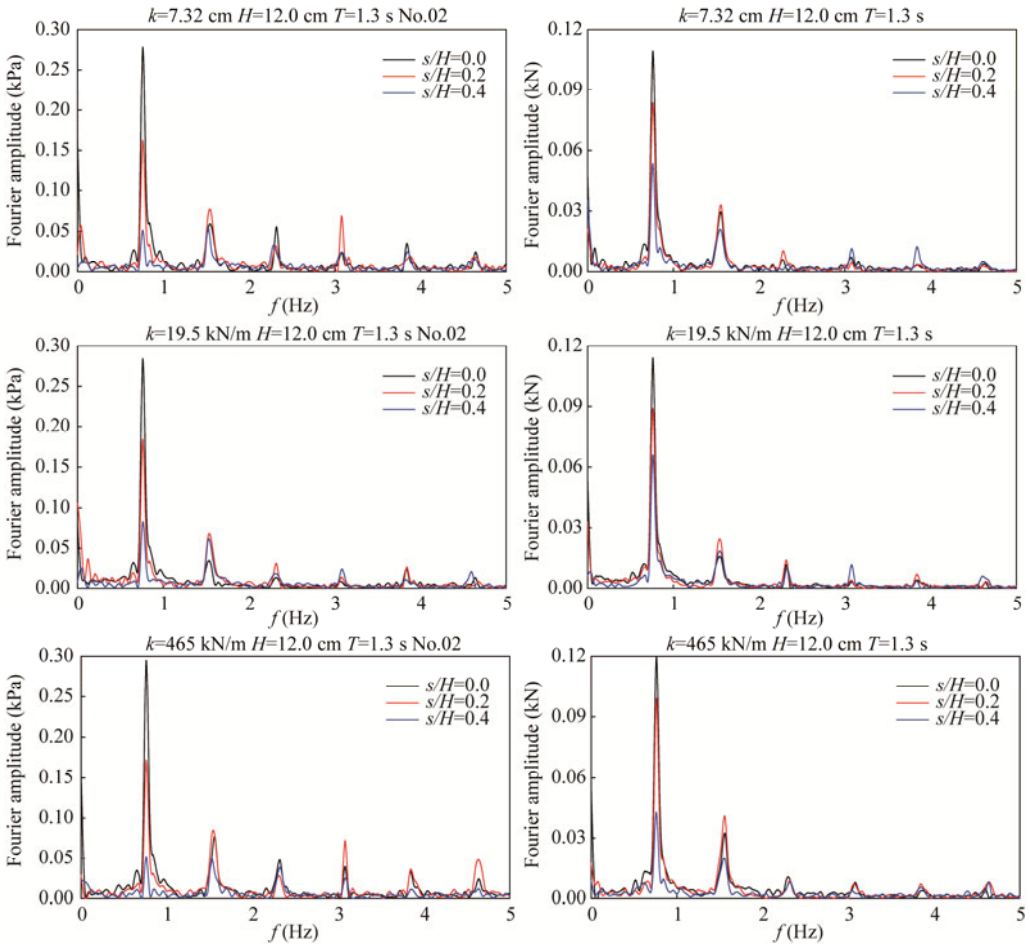

Fig. 9. Amplitude spectrums of the impact forces and pressures of P2 (T=1.3 s, H=12 cm).

According to the statistical analysis results in the time domain, the peak impact pressure (force) increases dramatically with the increase of the supporting stiffness. However, the spectral analysis results show that the spectral peaks increase a little with the increase of the support stiffness. Because of the properties of the impact pressures (forces), the duration of the peak pressures (forces) is very short and cannot be reflected by the spectral analysis, while the hydrodynamic pressures (forces) of longer duration are reflected in the spectral analysis. The hydrodynamic pressures decrease with the increase of the relative clearance of the structure and have little correlation with the limited movement response of the structure. Consequently the corresponding main spectral peak of the impact pressure (force) decreases as the relative clearance increases.

4. Conclusions

A series of model tests are performed to investigate the effect of hydro-elasticity on the impacting pressures. The experimental results indicate that different motion responses caused by wave impacting

result in different impacting loads on the structure with different support stiffness. The conclusions of those experiments are as follows.

(1) One impacting period can be divided into four stages. The duration of the impact pressures decreases with the increase of the supporting stiffness. For the model with larger stiffness, the oscillating amplitude of the acceleration is relatively small in each stage, whereas for the model with smaller stiffness, the acceleration oscillates more violently in each stage.

(2) The peak pressures distribute uniformly along the subface of the model with smaller stiffness (k=7.32 kN/m), whereas for the models with larger stiffness (k=19.5 kN/m and k=465 kN/m), the peak pressures of P2 and P3 on the seaward are obviously larger than those of the measured points on the shoreward.

(3) In these experiments the peak forces increase with the increase of the supporting stiffness for the same incident waves and clearance. For the models with larger stiffness (k=465 kN/m and k=19.5 kN/m), the maximum value of peak force occurs at s/H=0.1–0.2, which is similar to the rigid case. For the model with smaller stiffness (k=7.32 kN/m), the impact peak force is small and changes little with the change of the relative clearance.

(4) The spectral analysis results of the impacting pressures (forces) show that the maximum value of the main spectral peak at the incident frequency occurs at s/H=0.0, whereas the maximum value of the secondary peak at the double frequency occurs at s/H=0.2. The spectral peaks increase a little with the increase of the support stiffness. The main spectral peak of impact pressures (forces) decreases as the relative clearance increases.

References

Abramson, H. N., Bass, R. L., Faltinsen, O. M. and Olsen, H. A., 1976. Liquid slosh in LNG carriers, *The 10th International Symposium Proceedings*: *Naval Hydrodynamics*, Arlington, 371–388.

Baarholm, R. and Faltinsen, O. M., 2000. Experimental and theoretical studies of wave impact on an idealized platform deck, *Proc. 4th International Conference on Hydrodynamics*, Japan, 181–186.

Faltinsen, O. M. and Michelsen, F., 1975. Motions of large structures in wave at zero Froude number, *The International Symposium Proceedings: Dynamics of Marine Vehicles and Structures in Waves*, London, 91–106.

Faltinsen, O. M., Kjaerland, O., Nøttveit, A. and Vinje, T., 1977. Water impact loads and dynamic response of horizontal circular cylinders in offshore structures, *Proceedings of the 9th Annual Offshore Technology Conference*, Houston, USA, 2741, 119–126.

Faltinsen, O. M., 1997. The effect of hydroelasticity on ship slamming, *Philosophical Transactions of the Royal Society A*: *Mathematical*, *Physical and Engineering Sciences*, **355**(1724): 575–591.

Faltinsen, O. M., 1999. Water entry of a wedge by hydroelastic orthotropic plate theory, *Journal of Ship Research*, **43**(3): 180–193.

Faltinsen, O. M., 2000. Hydroelastic slamming, *Journal of Marine Science and Technology*, **5**(2): 49–65.

Faltinsen, O. M. and Timokha, A. N., 2009. *Sloshing*, Cambridge University Press.

Goda, Y., 1967. Wave forces on structures, *Summer Seminar on Hydraulics*, JSCE, Japan, B34.

Kaplan, P. and Silbert, M. N., 1976. Impact forces on platform horizontal members in the splash zone, *Proceedings of the 8th Annual Offshore Technology Conference*, Houston, USA, 2498, 749–758.

Kaplan, P., 1992. Wave impact force on offshore structures: Re-examination and new interpretations, *Proceedings of the 24th Annual Offshore Technology Conference*, USA, 6814, 79–86.

Korobkin, A. A. and Khabakhpasheva, T. I., 1999. Plane linear problem of the immersion of an elastic plate in an ideal incompressible fluid, *Journal of Applied Mechanics and Technical Physics*, **40**(3): 491–500.

Miller, B. L., 1978. Wave slamming loads on horizontal circular elements of offshore structures, *Journal Royal Institute Naval Architects*, **3**, 169–175.

Ren, B. and Wang, Y. X., 2004. Numerical simulation of random wave slamming on structures in the splash zone, *Ocean Eng*., **31**(5): 547–560.

Ren, B. and Wang, Y. X., 2005. Laboratory study of random wave slamming on a piled wharf with different shore connecting structures, *Coast. Eng*., **52**(5): 463–471.

Sarpkaya, T., 1978. Wave impact loads on cylinders, *Proceedings of the 10th Annual Offshore Technology Conference*, Houston, Texa, USA, 3065, 169–176.

Sulisz, W., Wilde, P. and Wisniewski, M., 2005. Wave impact on elastically supported horizontal deck, *Journal of Fluids and Structures*, **21**(3): 305–319.

Sumi, Y., Okada, S., Mukai, H. and Inoue, K., 1997. Study on water impact of elastic plate with small deadrise angles, *Journal of the Society of Naval Architects of Japan*, **182**, 639–646.

Tanizawa, K., 1998. A time-domain simulation method for hydroelastic impact problem, *Proceedings of the 2nd International Conference on Hydroelasticity in Marine Technology*, Fukuoka, Japan, 119–128.

von Kármán, T., 1929. *The Impact on Seaplane Floats During Landing*, National Advisory Committee for Aeronautics, Technical Notes 321.

Wagner, V. H., 1932. Über Stoß-und Gleitvorgänge an der Oberfläche von Flüssigkeiten, *Zeitschrift für Angewandte Mathematik und Mechanik*, **12**(4): 273–285. (in Germany)

Zhao, R., Faltinsen, O. M. and Aarsnes, J. V., 1996. Water entry of arbitrary two-dimensional sections with and without flow separation, *Proceedings of the 21st Symposium on Naval Hydrodynamics*, Washington, D.C., National Academy Press, 408–423.